Investigation of Size Dependence on Sensitivity for Nanowire FET Biosensors

Jae-Hyuk Ahn, Sung-Jin Choi, Jin-Woo Han, Tae Jung Park, Sang Yup Lee, and Yang-Kyu Choi

***Abstract*—Label-free electrical detection of biomolecules is demonstrated with a double-gate (DG) nanowire (NW) field-effect transistor (FET). Experimental results confirm that detection sensitivity is favorably improved by the increment of NW size in the DG-NWFET, whereas it is enhanced by the decrement of NW size in a conventional single-gate (SG) NWFET. Sensitivity improvement by the augmentation of the NW size in the DG-FET paves the way to overcome technical challenges we face in achieving ultimate miniaturization of the NW size in the SG-FET. This result is comprehensively understood by simple capacitive modeling. The proposed model explains the observed experimental data and provides a design guideline for highly sensitive NW biosensors.**

***Index Terms*—Biosensor, capacitive model, double gate (DG), field-effect transistor (FET), nanowire (NW).**

I. Introduction

BIOSENSORS using a nanowire (NW) field-effect transistor (FET) have great potential in label-free detection of biomolecules at ultralow concentration [1]–[6]. Charged molecules bound to NW surfaces lead to carrier modulation (depletion or accumulation) in the NW, resulting in a current change [7], [8]. A field gating through a solution medium due to charges from the bound molecules can strongly affect the channel potential in an NW device, whereas it has less influence on the channel potential in a bulky device [9]. As a consequence, the detection sensitivity is significantly improved by the reduction of the NW size. It is well known that sensitivity is enhanced as the ratio of surface to volume is increased; hence, many pieces of research have been carried out to fabricate NWs to be as small as possible [8], [9]. Many applications have been demonstrated for sensing DNA [5], [10]–[12], proteins [6], [13], small molecules [14], and viruses [15] by full utilization of the benefits arising from the nature of small NW devices.

There have been two approaches in forming an NW: top down and bottom up [16]. The top-down approach suffers from a lithographic resolution limit, even though it allows control of the position and shape of the NW with high throughput. However, the bottom-up approach suffers difficulty in managing the position and shape of the NW, although it can reduce the size of the NW beyond the limit of the lithographic resolution. Thus, it is timely to consider structural and/or operational modification to overcome these challenges. Additionally, it is attractive to utilize the well-established infrastructure of CMOS technology for mass production to take advantages of its low cost, approved reliability, and reproducibility. On the other hand, it is also important to sustain the properties of CMOS compatibility for biosensor fabrication because the circuitry for the decoder, readout, and signal processing is composed of CMOS devices.

To overcome the scaling limit in the aforementioned miniaturization, structural or operational modification is necessary to find a shortcut to a new method. One of the structural modifications that have been proposed was to reduce the dimensionality from three-dimension (3-D, bulky device) to two-dimension (2-D, nanoribbon) by reducing the channel thickness while relieving the pressure in the miniaturization of the channel width, which was defined by photolithography [17]. Similarly, proposed operational alteration transferred the sensing domain from the threshold domain or beyond to the subthreshold domain [18]. Thus, sensitivity was improved without risking the ultimate downscaling. On the other hand, both of these approaches to structural modification and operational modification used a moderate-sized double-gate NWFET (DG-NWFET), which was delineated by commercialized top-down photolithography [19], [20]. Specifically, the structural modification was completed by employment of the separated DG straddling both the sidewalls of the silicon NW, while the operational modification was achieved by using an asymmetrically operating gate bias applied to each gate electrode.

In this paper, comprehensive capacitive modeling is carried out to analytically explain a new approach in which a larger size ensures more sensitivity and to understand the underlying

Manuscript received March 11, 2011; revised May 12, 2011; accepted May 13, 2011. Date of publication May 27, 2011; date of current version November 9, 2011. This work was supported in part by the Center for Nanoscale Mechatronics and Manufacturing, one of the 21st Century Frontier Research Programs supported by the Korea Ministry of Education, Science and Technology (MEST), under Grant 08K1401-00210, in part by the National Research and Development Program for the development of biomedical function monitoring biosensors under Grant 2011-0002182, and in part by the National Research Foundation of Korea funded by the Korean government under Grant 2010-0018931. The review of this paper was arranged by Associate Editor B. Nelson.

J.-H. Ahn, S.-J. Choi, and Y.-K. Choi are with the Department of Electrical Engineering, Korea Advanced Institute of Science and Technology, Daejeon 305-701, Korea (e-mail: jhahn@nobelab.kaist.ac.kr; sjchoi@nobelab.kaist.ac.kr; ykchoi@ee.kaist.ac.kr).

J.-W. Han is with the Center for Nanotechnology, NASA Ames Research Center, Moffett Field, CA 94035 USA (e-mail: jin-woo.han@nasa.gov).

T. J. Park is with the BioProcess Engineering Research Center, Center for Systems and Synthetic Biotechnology, Institute for the BioCentury, Korea Advanced Institute of Science and Technology, Daejeon 305-701, Korea (e-mail: tjpark@kaist.ac.kr).

S. Y. Lee is with the BioProcess Engineering Research Center, Center for Systems and Synthetic Biotechnology, Institute for the BioCentury, KAIST, Daejeon 305-701, Korea, and also with the Department of Chemical and Biomolecular Engineering, the Department of Biological Sciences, the Department of Bio and Brain Engineering, and Bioinformatics Research Center, KAIST, Daejeon 305-701, Korea (e-mail: leesy@kaist.ac.kr).

Color versions of one or more of the figures in this paper are available online at http://ieeexplore.ieee.org.

Digital Object Identifier 10.1109/TNANO.2011.2157519

1536-125X/$26.00 © 2011 IEEE

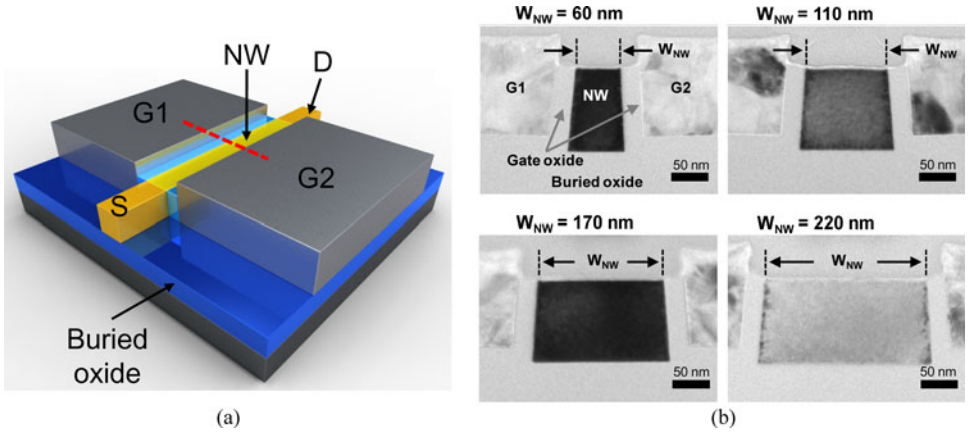

Fig. 1. (a) Schematic to show a DG-NWFET with each bias condition from a bird's eye view. An NW is formed on the buried oxide, and two gates ($G1$ and $G2$) straddle the NW at each side. To measure the drain current–gate voltage (I_D–V_G) characteristics, a source (S) is grounded and a drain (D) is biased to low drain voltage (V_D) with 50 mV. The same bias is applied to $G1$ and $G2$, resulting in a symmetrical sweep ($V_{G1} = V_{G2}$). The top surface of the NW is open to immobilize biomolecules. (b) Cross-sectional TEM images along the dashed line in (a). The widths of the NW are in a range of 60–220 nm.

principle. This simple and comprehensive model calibrated by experimental data can provide a guideline for designing highly sensitive sensors.

II. Experiment

The DG-NWFETs were fabricated with the top-down approach that was previously reported by our group [19]. The device schematic and TEM images of the fabricated device are shown in Fig. 1(a) and (b), respectively. Details of the process flow were also described in the same paper. Two solid-state gate electrodes (denoted as $G1$ and $G2$) are separated from each other. Thus, not only a symmetrical bias ($V_{G1} = V_{G2}$), but also an asymmetrical bias ($V_{G1} \neq V_{G2}$) is possible to modulate the electron conduction. Unlike a device covered by native oxide, which is usually grown in an air environment, here the top surface of the NW is covered by thermally grown oxide with a 3 nm thickness to improve the yield in immobilization of the biomolecules.

For electrical characterization, the source is grounded in all measurements. Drain current–gate voltage (I_D–V_G) measurements were taken with a gate voltage sweep at a low drain voltage of 50 mV. The two gates are tied and the same bias is applied to the gates for the symmetrical operation ($V_{G1} = V_{G2} = V_G$). Under the condition of threshold voltage V_T, inversion electrons are induced and I_D starts to flow. V_T is read when I_D is 10 nA [21].

To demonstrate the sensing ability of the DG-NWFETs, the antigen and antibody of the avian influenza (AI) virus were used as test materials. The surface antigen of AI (AIa) was fused with a specifically designed protein, called the silica binding protein (SBP), which can be immobilized on the top surface of the NW in the DG-NWFETs without extra surface treatment. Details of SBP design and immobilization procedures were reported elsewhere [22]–[24]. SBP-AIa, a protein fused with SBP and AIa, can be bound to the antibody against AI (anti-AI), as shown in Fig. 2(a). For immobilization of SBP-AIa on the NW, the device was incubated in a 25 μg/mL solution of SBP-AIa in a phosphate-buffered saline (PBS, pH 7.4) solution for 1 h. Then,

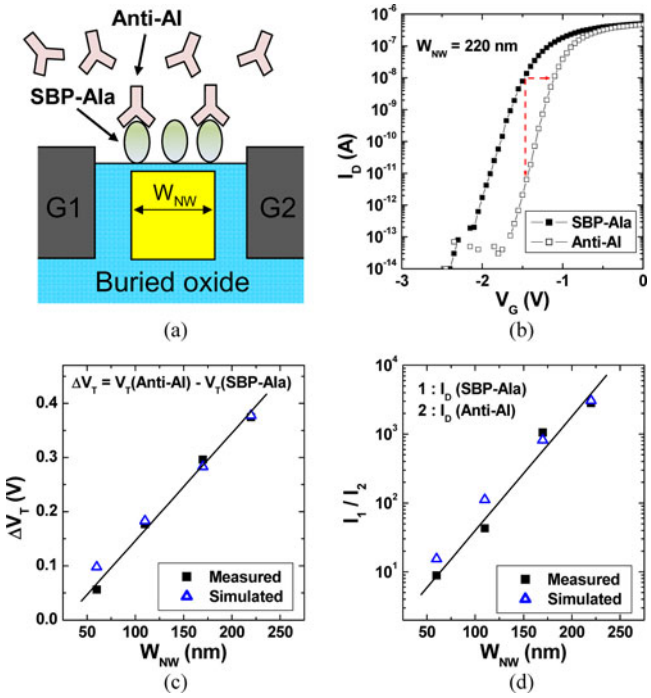

Fig. 2. (a) Schematic to show the cross-sectional view of the DG-NWFET and biomolecules interacting on the NW. The antibody of the AI (anti-AI) binds to SBP-AIa, which is a fusion protein including an SBP) and AIa. (b) Measured I_D after SBP-AIa immobilization (filled squares) and subsequent anti-AI binding (hollow squares). V_T is increased and I_D is reduced because anti-AI is a negatively charged biomolecule. (c) Measured V_T shift (black squares) versus the width of the NW in a range of 60–220 nm. Blue triangles show the simulated V_T shift for the corresponding widths. (d) I_D ratio before and after anti-AI binding versus the width of the NW in a range of 60–220 nm. Blue triangles show the simulated I_D ratio for the corresponding widths.

the device was rinsed several times with deionized water and blown dry with nitrogen before electrical measurement. The binding experiments were performed by incubating the SBP-AIa-immobilized device in a 20 μg/mL solution of anti-AI in the PBS solution for 1 h, followed by washing and drying in the same way. All incubations were performed at room temperature.

It is worthwhile to note that all electrical measurements were performed after removing the buffer solution and deionized water from the device by nitrogen blowing, which was also used in other studies [11]. This state can be considered as a "quasi-wet" state, which implies that the fundamental properties of the biomolecules, such as intrinsic charge and specificity, are still sustained. After the last nitrogen blowing, all the electrical measurements were carried out within 1 h, which is the warranted time to show that there was no significant change of electrical characteristics as time passed. According to previous results, the characteristics of biomolecules can be maintained stably for more than 5 h [23].

In the FET biosensor, there were two well-known metrics: drain current I_D relevant to conductance g_m and threshold voltage V_T. The specific binding of a capture and a target biomolecule can be detected by keeping track of the change of those metrics. When the negatively charged anti-AI was bound to SBP-AIa, which had adhered to the top surface of the NW, I_D decreased and V_T increased in the n-channel FET, as shown in Fig. 2(b), which is consistent with previous work [19]. It should be noted that the change of metrics, I_D and V_T, is affected by the width of the NW, W_{NW}. Fig. 2(c) and (d) shows the tendency that a wider dimension gives rise to more changes of both of the metrics. Moreover, Fig. 2(d) clearly explains that the signal-to-noise ratio, which is defined as the I_D ratio before and after the anti-AI binding, is improved as W_{NW} is increased. The measured data show good agreement with the simulation data, which were produced by a semiconductor simulation tool (ATLAS of SILVACO, Inc., CA) to support a 3-D device structure [25]. Interestingly, this is opposite to the traditional result that a wider NW showed a weaker response, which was reported by other researchers [9], [26].

III. Analytical Model

An analytical model is proposed to explain our findings, i.e., the tendency that a wider dimension shows an improved sensitivity. If this model is applied to the previously reported 1-D NW and 2-D nanoribbon, its validity can also be verified. There have been several approaches to developing a proper model to explain the measured characteristics from FET devices, such as a current–voltage model [27], a potential model [28], and a capacitive model [20]. Among them, the capacitive model is suitable for characterization of FET biosensors because it is valid even in a subthreshold or depleted regime where the sensors show the maximum sensitivity [18]. Moreover, it is the simplest method for providing physical insights considering geometric and bias effects influencing sensitivity.

As shown in Fig. 3(a), the suggested capacitive model for the DG-NWFET is overlaid with the cross-sectional schematic along the gate direction, which is perpendicular to the source–drain direction. The model is composed of several capacitances, which are the gate capacitance C_G, the capacitance of the thin oxide on the top surface of the NW for sensing target biomolecules C_{sens}, and the NW capacitances $C_{\mathrm{Si},1}$ and $C_{\mathrm{Si},2}$ located on top and inside of the NW, respectively. Based on the simulation results, we treat the NW capacitance as the depletion capacitance [21] stemming from depletion of electrons. All details of the equations for corresponding capacitances are summarized in Table I. Unlike the work by Knofmacher *et al.* [20], each capacitance explicitly includes geometrical parameters such as oxide thickness and NW size.

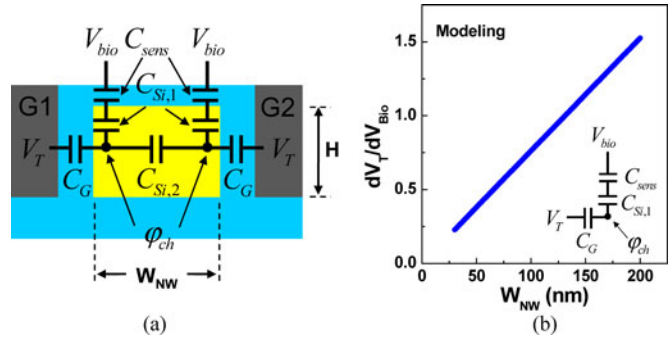

Fig. 3. (a) Capacitive model of the DG-NWFET along the direction of the gates. An electrical channel, in which its potential denotes φ_{ch}, is located on both sides of the gates. C_G denotes the gate and C_{sens} the top oxide capacitance. $C_{\mathrm{Si},1}$ and $C_{\mathrm{Si},2}$ are the horizontal and vertical capacitances inside the NW, respectively, stemming from depletion of the carriers. (b) Calculated dV_T/dV_{bio} from the model suggested in (2) versus the NW widths. The inset shows a simplified capacitive model of the DG-NWFET.

TABLE I
Capacitances and Their Representations Used in the Capacitive Model

Capacitance	Value
C_{sens}	$\varepsilon_{SiO_2} \cdot \left(W_{NW}/2 \big/ t_{ox} \right) \cdot L_G$
C_G	$\varepsilon_{SiO_2} \cdot \left(H \big/ t_G \right) \cdot L_G$
$C_{Si,1}$	$\varepsilon_{Si} \cdot \left(W_{NW} \big/ H \right) \cdot L_G$
$C_{Si,2}$	$\varepsilon_{Si} \cdot \left(H \big/ W_{NW} \right) \cdot L_G$

The permittivity of SiO_2 ε_{SiO2} and permittivity of silicon ε_{Si} are 3.45×10^{-13} and 1.04×10^{-12} F/cm, respectively. The thickness of the gate oxide t_G is 30 nm. Oxide thickness at the top surface of the NW t_{ox} is 3 nm and it inhibits electrical short between the NW channel and immobilized biomolecules. L_G is the gate length of 1 μm. W_{NW} and H are the width and height of the DG-NWFET.

The channel is induced by applied gate bias. The potential of the channel is denoted as φ_{ch}, which is affected by gate voltage and the charged biomolecules. As mentioned earlier, V_T is defined when the device is operating at the subthreshold regime. The quantity of the charges in the biomolecules induces a certain amount of surface potential V_{bio} onto the top surface of the NW; hence, it gives rise to change V_T. Thus, the sensitivity can be taken as a quantity of how much V_T is changed by V_{bio}. The sensitivity, which is a dimensionless parameter, can be represented by

$$\frac{dV_T}{dV_{\mathrm{bio}}} = \frac{dV_T}{d\varphi_{\mathrm{ch}}} \cdot \frac{d\varphi_{\mathrm{ch}}}{dV_{\mathrm{bio}}}. \tag{1}$$

Equation (1) is simply divided into two coupling ratios. One coupling ratio between the channel and the biomolecules is $d\varphi_{\rm ch}/dV_{\rm bio}$. The other coupling ratio between the channel and the gates is $d\varphi_{\rm ch}/dV_T$ under the V_T condition ($V_G = V_T$).

The model presented in Fig. 3(a) can be simplified as shown in the inset of Fig. 3(b), considering only the capacitances connected with $V_{\rm bio}$, V_T, and $\varphi_{\rm ch}$. As shown in Fig. 3(a), the same $\varphi_{\rm ch}$ is symmetrically applied to both sides of $C_{\rm Si,2}$; hence, $C_{\rm Si,2}$ can be ignored when calculating the coupling ratios. As presented in the inset of Fig. 3(b), $d\varphi_{\rm ch}/dV_T$ is relevant to C_G, whereas $d\varphi_{\rm ch}/dV_{\rm bio}$ is associated with $(1/C_{\rm sens} + 1/C_{\rm Si,1})^{-1}$ because of its serial connection. Thus, the sensitivity under the symmetrical bias condition is rewritten as

$$\frac{dV_T}{dV_{\rm bio}} = \frac{(1/C_G)}{((1/C_{\rm sens}) + (1/C_{\rm Si,1}))}. \tag{2}$$

The calculated sensitivity from the model in (2) is shown in Fig. 3(b). It clearly shows that the sensitivity ($dV_T/dV_{\rm bio}$) increases as $W_{\rm NW}$ increases. It should be noted that this arises from the increased coupling ratio ($d\varphi_{\rm ch}/dV_{\rm bio}$) between the channel and the biomolecules because both $C_{\rm sens}$ and $C_{\rm Si,1}$ are linearly increased by an increment of $W_{\rm NW}$, as shown in Table I.

Enhanced sensitivity can be achieved using an asymmetric bias condition ($V_{G1} \neq V_{G2}$) in which $G1$ is used as a sensing gate that monitors the change in V_T when the biomolecules are changed, and $G2$ is used as a supporting gate that modulates the conduction path of the electrons for sensitivity enhancement [19]. As shown in Fig. 4(a), one voltage V_T is applied to $G1$ and another voltage larger than V_T is applied to $G2$. Thus, a primary conduction path (or inversion layer) is created only on the $G2$ side. Under this condition, $d\varphi_{\rm ch}/dV_T$ is related to $(1/C_G + 1/C_{\rm Si,2})^{-1}$. Note also, as shown in Fig. 4(b), that $C_{\rm Si,2}$ is not ignorable when the coupling effects are induced under the asymmetrical bias condition. The sensitivity is, therefore, changed to

$$\frac{dV_{T,\rm asym}}{dV_{\rm bio}} = \frac{((1/C_G) + (1/C_{\rm Si,2}))}{((1/C_{\rm sens}) + (1/C_{\rm Si,1}))}. \tag{3}$$

As shown in Fig. 4(c), the sensitivity is dramatically better than that of the symmetrically biased device ($V_{G1} = V_{G2}$) when $W_{\rm NW}$ is increased. This additional sensitivity improvement essentially comes from the fact that the coupling ratio between the channel and the gate ($d\varphi_{\rm ch}/dV_T$) is decreased by the reduction of $C_{\rm Si,2}$ when $W_{\rm NW}$ is increased. The comparison between the modeled data and the measured data shown in Fig. 4(d) validates the trend predicted by the proposed model.

From the capacitive model, the newly found trend that a larger size shows a more improved sensitivity is comprehensively understood even though it is oppose to the tendency observed in other devices: the conventional single-gate NW [9], [26] and nanoribbon [17] FET biosensor. To find the reasons for this opposite trend, a similar capacitive modeling is carried out for the NW and nanoribbon FET schematically depicted in Fig. 5(a). Actually, those devices are almost equivalent to each other because the NW is changed to a nanoribbon when its width becomes much larger than its thickness. A schematic of the capacitive model is presented in Fig. 5(b) with each subcapacitance in their cross section. This approach can be applied to both the NW (1-D) and nanoribbon (2-D) FET, simultaneously. As shown in Fig. 5(b), the total capacitance comprises the gate capacitance $C_{G,1}$, the thin oxide capacitance for sensing target biomolecules $C_{\rm sens,1}$ on the top surface and $C_{\rm sens,2}$ on the side surface of the NW, as well as the NW capacitances $C_{\rm Si,1}$ and $C_{\rm Si,2}$, which are inside the NW. Their corresponding values of capacitances are summarized in Table II. In the case of the NWFET biosensor, the lateral capacitance, which is a serial connection of $C_{\rm sens,2}$ and $C_{\rm Si,2}$, is more dominant than the vertical capacitance, a serial connection of $C_{\rm sens,1}$ and $C_{\rm Si,1}$, as the NW width ($W_{\rm NW}$) is decreased. The model is simplified as shown in the inset of Fig. 5(c). From the simple calculation of the capacitances, $d\varphi_{\rm ch}/dV_T$ and $d\varphi_{\rm ch}/dV_{\rm bio}$ are obtained with $C_{G,1}$ and $(2/C_{\rm sens,2} + 2/C_{\rm Si,2})^{-1}$, respectively. According to (1), the sensitivity $dV_T/dV_{\rm bio}$ is given by

$$\frac{dV_T}{dV_{\rm bio}} = \frac{(1/C_{G,1})}{2\left((1/C_{\rm sens,2}) + (1/C_{\rm Si,2})\right)}. \tag{4}$$

As shown in Fig. 5(c), the sensitivity decreases as the device dimension, namely, the NW width ($W_{\rm NW}$) increases. In other words, as the size of the NW increases, the sensitivity

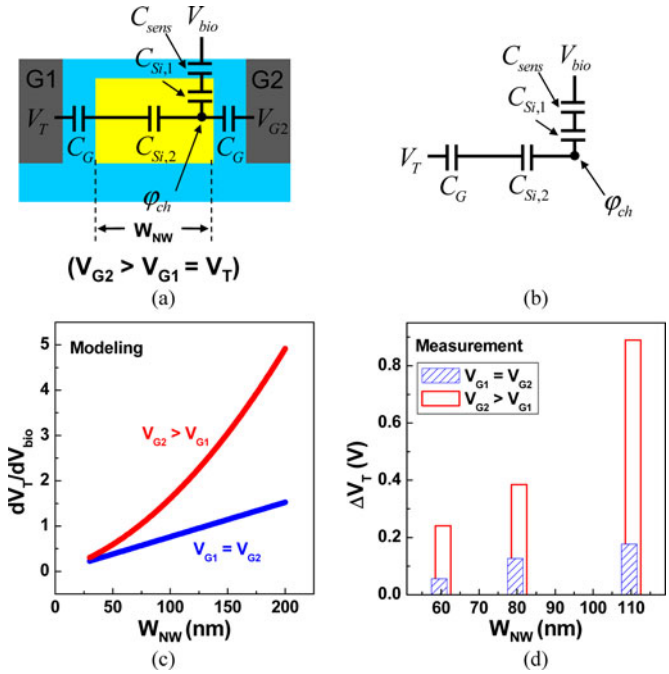

Fig. 4. (a) Capacitive model of a DG-NWFET along the direction of gates in an asymmetrical mode ($V_{G1} \neq V_{G2}$). The electrical channel, the potential of which is denoted by $\varphi_{\rm ch}$, is located only on the $G2$ side, where $V_{G2} > V_T$. The term C_G denotes the gate capacitance and the term $C_{\rm sens}$ denotes the top oxide capacitance used in the sensing of the biomolecules. The terms $C_{\rm Si,1}$ and $C_{\rm Si,2}$ are the horizontal and vertical capacitances inside the NW, respectively. (b) Simplified capacitive model for determining the sensitivity $dV_T/dV_{\rm bio}$ which is expressed in (3). (c) Calculated value of $dV_T/dV_{\rm bio}$ versus the NW widths under different operational modes. The blue and red lines show the modeled data for the symmetrical mode (2) and the asymmetrical mode (3), respectively. (d) Measured V_T shift versus the NW widths under different operational modes.

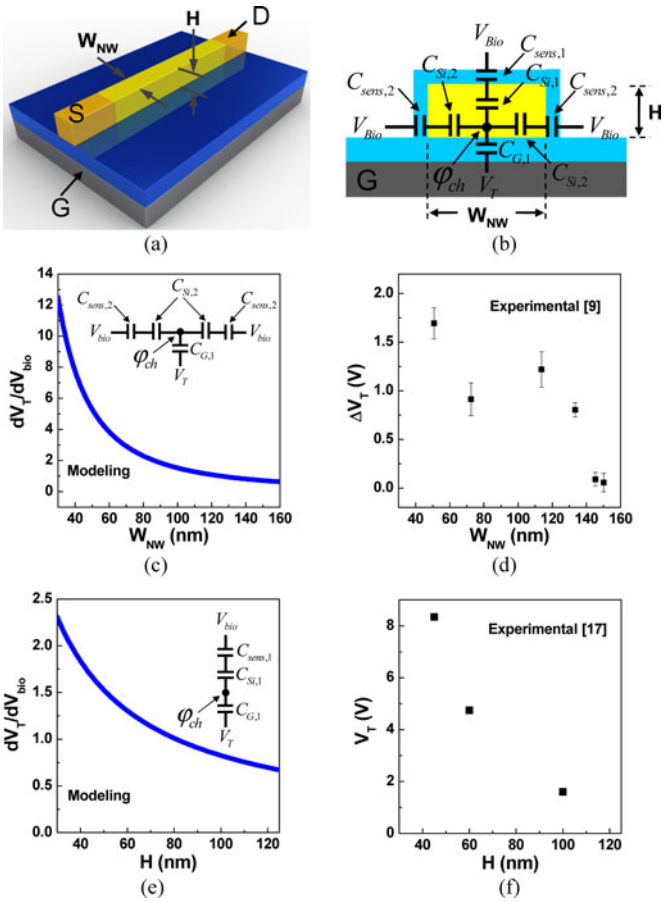

Fig. 5. (a) Schematic to show an NW or nanoribbon FET from a bird's eye view. The width is much larger than the height in the nanoribbon. (b) Capacitive model of the NW and nanoribbon along the direction of the gates. $C_{G,1}$ denotes the gate, $C_{\mathrm{sens},1}$ the top oxide, and $C_{\mathrm{sens},2}$ the side oxide capacitance. $C_{\mathrm{Si},1}$ and $C_{\mathrm{Si},2}$ are the horizontal and vertical capacitances inside the NW, respectively, stemming from depletion of the carriers. (c) Calculated dV_T/dV_{bio} from the model suggested in (4) versus the various NW widths. The inset shows a simplified capacitive model of the NW. (d) Measured V_T shift [9] versus the NW widths. (e) Calculated dV_T/dV_{bio} from the model suggested in (5) versus the nanoribbon heights. The inset shows a simplified capacitive model of the nanoribbon. (f) Measured V_T [17] versus the nanoribbon heights.

represented by dV_T/dV_{bio} is reduced because $d\varphi_{\mathrm{ch}}/dV_{\mathrm{bio}}$ is reduced with an increased $C_{G,1}$ and $d\varphi_{\mathrm{ch}}/dV_T$ is increased with a reduced $C_{\mathrm{Si},2}$. Such a predictive trend from the capacitive model shows good agreement with the experimental data [9] as shown in Fig. 5(d).

A similar capacitive modeling is carried out for the nanoribbon FET biosensor. Since the nanoribbon width is in the range of a micrometer scale, the lateral capacitance can be ignored. The gate capacitance and vertical capacitance, which is composed of $C_{\mathrm{sens},1}$ and $C_{\mathrm{Si},1}$, remain as shown in the inset of Fig. 5(e). $d\varphi_{\mathrm{ch}}/dV_T$ and $d\varphi_{\mathrm{ch}}/dV_{\mathrm{bio}}$ are calculated with $C_{G,1}$ and $(1/C_{\mathrm{sens},1} + 1/C_{\mathrm{Si},1})^{-1}$, respectively. According to (1), the sensitivity dV_T/dV_{bio} is defined by

$$\frac{dV_T}{dV_{\mathrm{bio}}} = \frac{(1/C_{G,1})}{((1/C_{\mathrm{sens},1}) + (1/C_{\mathrm{Si},1}))}. \tag{5}$$

As shown in Fig. 5(e), the sensitivity decreases as NW height H increases. An increment of H lowers $d\varphi_{\mathrm{ch}}/dV_{\mathrm{bio}}$ because $C_{\mathrm{Si},1}$ is reduced, and thus, dV_T/dV_{bio} is reduced. The trend of this result according to H is well matched with experimental results [17] as shown in Fig. 5(f). As a result, this capacitive model can be universally applied for the NW and nanoribbon FET as well as the DG-NWFET.

TABLE II
CAPACITANCES AND THEIR REPRESENTATIONS USED IN THE CAPACITIVE MODEL

Capacitance	Value
$C_{sens,1}$	$\varepsilon_{SiO_2} \cdot \left(W_{NW} / t_{ox} \right) \cdot L_G$
$C_{sens,2}$	$\varepsilon_{SiO_2} \cdot \left(H/2 / t_{ox} \right) \cdot L_G$
$C_{G,1}$	$\varepsilon_{SiO_2} \cdot \left(W_{NW} / t_G \right) \cdot L_G$
$C_{Si,1}$	$\varepsilon_{Si} \cdot \left(W_{NW} / H \right) \cdot L_G$
$C_{Si,2}$	$\varepsilon_{Si} \cdot \left(H / W_{NW} \right) \cdot L_G$

Permittivity of SiO_2 ε_{SiO2} and permittivity of silicon ε_{Si} are 3.45×10^{-13} and 1.04×10^{-12} F/cm, respectively. The thickness of the gate oxide t_G is 30 nm. Oxide thickness at the top and sidewall surface of the NW t_{ox} is 3 nm. L_G is the gate length of 1 μm. W_{NW} and H are the width and height of the NW and the nanoribbon device, respectively.

Most of the NW biosensors have micrometer-sized gate lengths even though the width of the NW is extremely narrow. It is free from short-channel effects (SCEs), which are mostly shown in the submicrometer gate length. SCEs degrade the device performance and change the value of device performance parameters such as threshold voltage V_T, subthreshold swing, and drain-induced barrier lowering. In this micrometer regime, however, it is well known that the gate length does not significantly affect device performance parameters [21]. Thus, this can support that the sensitivity (dV_T/dV_{bio}) is independent of the gate length.

According to (1), it is attractive to enhance the sensitivity by maximizing $d\varphi_{\mathrm{ch}}/dV_{\mathrm{bio}}$ and minimizing $d\varphi_{\mathrm{ch}}/dV_T$. As a consequence, different scaling strategies should be applied to DG-NWFETs and conventional NWFETs: a widened NW for DG-NWFETs and a narrowed NW or thin nanoribbon for conventional NWFETs.

There are more degrees of freedom in the process integration when a large-sized feature is allowed for a sensor compared to when only a small one is permitted, without sacrifice of the sensitivity. Therefore, pressure from ultimate miniaturization can be relieved, the process flow can be simplified, and the cost can be cut. Moreover, it had been reported that the total analyte flux is enhanced when sensor size is increased; thus, one can overcome the analyte transport limitation, which makes it difficult to attain the subpicomolar sensitivity in a nanoscale sensor on a relevant time scale [29].

IV. Conclusion

We have presented a new strategy that confirms that a large size results in greater sensitivity in DG-NWFETs. That trend was experimentally demonstrated and verified using a capacitive model. The trend was further validated by the use of a commercialized semiconductor simulation tool. The pressure to push the sensor size to a fundamental limit in patterning was alleviated by the structural and operational modification of the pre-existing NW FET after implementation of the DG with the aid of a conventional CMOS process. Thus, this approach can pave the way to produce low cost and reliable biosensors. The proposed capacitive model can provide a guideline in designing their architecture and operational conditions.

References

[1] Y. Cui, Q. Wei, H. Park, and C. M. Lieber, "Nanowire nanosensors for highly sensitive and selective detection of biological and chemical species," *Science*, vol. 293, pp. 1289–1292, Aug. 2001.

[2] R. J. Chen, S. Bangsaruntip, K. A. Drouvalakis, N. W. S. Kam, M. Shim, Y. Li, W. Kim, P. J. Utz, and H. Dai, "Noncovalent functionalization of carbon nanotubes for highly specific electronic biosensors," *Proc. Nat. Acad. Sci. U.S.A.*, vol. 100, pp. 4984–4989, Apr. 2003.

[3] A. Star, J.-C. P. Gabriel, K. Bradley, and G. Grüner, "Electronic detection of specific protein binding using nanotube FET devices," *Nano Lett.*, vol. 3, pp. 459–463, Apr. 2003.

[4] K. Besteman, J.-O Lee, F. G. M. Wiertz, H. A. Heering, and C. Dekker, "Enzyme-coated carbon nanotubes as single-molecule biosensors," *Nano Lett.*, vol. 3, pp. 727–730, Jun. 2003.

[5] J. Hahm and C. M. Lieber, "Direct ultrasensitive electrical detection of DNA and DNA sequence variations using nanowire nanosensors," *Nano Lett*, vol. 4, pp. 51–54, Jan. 2004.

[6] G. Zheng, F. Patolsky, Y. Cui, W. U. Wang, and C. M. Lieber, "Multiplexed electrical detection of cancer markers with nanowire sensor array," *Nat. Biotechnol.*, vol. 23, pp. 1294–1301, Oct. 2005.

[7] A. B. Artyukhin, M. Stadermann, R. W. Friddle, P. Stroeve, O. Bakajin, and A. Noy, "Controlled electrostatic gating of carbon nanotube FET devices," *Nano Lett.*, vol. 6, pp. 2080–2085, Sep. 2006.

[8] A. Kim, C. S. Ah, H. Y. Yu, J.-H. Yang, I.-B. Baek, C.-G. Ahn, C. W. Park, M. S. Jun, and S. Lee, "Ultrasensitive, label-free, and real-time immunodetection using silicon field-effect transistors," *Appl. Phys. Lett.*, vol. 91, p. 103901, Sep. 2007.

[9] N. Elfström, R. Juhasz, I. Sychugov, T. Engfeldt, A. E. Karlström, and J. Linnros, "Surface charge sensitivity of silicon nanowires: Size dependence," *Nano Lett.*, vol. 7, pp. 2608–2612, Sep. 2007.

[10] Z. Li, Y. Chen, T. I. Kamins, K. Nauka, and R. S. Williams, "Sequence-specific label-free DNA sensors based on silicon nanowires," *Nano Lett.*, vol. 4, pp. 245–247, Feb. 2004.

[11] A. Star, E. Tu, J. Niemann, J.-C. P. Gabriel, C. S. Joiner, and C. Valcke, "Label-free detection of DNA hybridization using carbon nanotube network field-effect transistors," *Proc. Nat. Acad. Sci. U.S.A.*, vol. 103, pp. 921–926, Jan. 2006.

[12] Y. L. Bunimovich, Y. S. Shin, W.-S. Yeo, M. Amori, G. Kwong, and J. R. Heath, "Quantitative real-time measurements of DNA hybridization with alkylated nonoxidized silicon nanowires in electrolyte solution," *J. Amer. Chem. Soc*, vol. 128, pp. 16323–16331, Dec. 2006.

[13] C. Li, M. Curreli, H. Lin, B. Lei, F. N. Ishikawa, R. Datar, R. J. Cote, M. E. Thompson, and C. Zhou, "Complementary detection of prostate-specific antigen using In_2O_3 nanowires and carbon nanotubes," *J. Amer. Chem. Soc.*, vol. 127, pp. 12484–12485, Sep. 2005.

[14] W. U. Wang, C. Chen, K.-h. Lin, Y. Fang, and C. M. Lieber, "Label-free detection of small-molecule–protein interactions by using nanowire nanosensors," *Proc. Nat. Acad. Sci. U.S.A.*, vol. 102, pp. 3208–3212, Mar. 2005.

[15] F. Patolsky, G. Zheng, O. Hayden, M. Lakadamyali, X. Zhuang, and C. M. Lieber, "Electrical detection of single viruses," *Proc. Nat. Acad. Sci. U.S.A.*, vol. 101, pp. 14017–14022, Sep. 2004.

[16] B. Bhushan and Ed, *Springer Handbook of Nanotechnology*. Heidelberg, Germany: Springer-Verlag, 2004.

[17] N. Elfström, A. E. Karlström, and J. Linnros, "Silicon nanoribbons for electrical detection of biomolecules," *Nano Lett.*, vol. 8, pp. 945–949, Mar. 2008.

[18] X. P. A. Gao, G. Zheng, and C. M. Lieber, "Subthreshold regime has the optimal sensitivity for nanowire FET biosensors," *Nano Lett.*, vol. 10, pp. 547–552, Feb. 2010.

[19] J.-H. Ahn, S.-J. Choi, J.-W. Han, T. J. Park, S. Y. Lee, and Y.-K. Choi, "Double-gate nanowire field effect transistor for a biosensor," *Nano Lett.*, vol. 10, pp. 2934–2938, Aug. 2010.

[20] O. Knopfmacher, A. Tarasov, W. Fu, M. Wipf, B. Niesen, M. Calame, and C. Schönenberger, "Nernst limit in dual-gated Si-nanowire FET sensors," *Nano Lett.*, vol. 10, pp. 2268–2274, Jun. 2010.

[21] S. M. Sze, *Physics of Semiconductor Devices*, 2nd ed. ed. New York: Wiley, 1981.

[22] K. Taniguchi, K. Nomura, Y. Hata, T. Nishimura, Y. Asami, and A. Kuroda, "The Si-tag for immobilizing proteins on a silica surface," *Biotechnol. Bioeng.*, vol. 96, pp. 1023–1029, Apr. 2007.

[23] S. Kim, J.-H. Ahn, T. J. Park, S. Y. Lee, and Y.-K. Choi, "A biomolecular detection method based on charge pumping in a nanogap embedded field-effect-transistor biosensor," *Appl. Phys. Lett.*, vol. 94, p. 243903, Jun. 2009.

[24] B. Gu, T. J. Park, J.-H. Ahn, X.-J. Huang, S. Y. Lee, and Y.-K. Choi, "Nanogap field-effect transistor biosensors for electrical detection of avian influenza," *Small*, vol. 5, pp. 2407–2412, Nov. 2009.

[25] *Atlas User's Manual*. Silvaco Int., Santa Clara, CA, 2008.

[26] E. Stern, J. F. Klemic, D. A. Routenberg, P. N. Wyrembak, D. B. Turner-Evans, A. D. Hamilton, D. A. LaVan, T. M. Fahmy, and M. A. Reed, "Label-free immunodetection with CMOS-compatible semiconducting nanowires," *Nature*, vol. 445, pp. 519–522, Feb. 2007.

[27] Y. Taur, X. Liang, W. Wang, and H. Lu, "A continuous, analytic drain-current model for DG MOSFETs," *IEEE Electron Device Lett.*, vol. 25, no. 2, pp. 107–109, Feb. 2004.

[28] K. Suzuki, T. Tanaka, Y. Tosaka, H. Horie, and Y. Arimoto, "Scaling theory for double-gate SOI MOSFET's," *IEEE Trans. Electron Devices*, vol. 40, no. 12, pp. 2326–2329, Dec. 1993.

[29] P. E. Sheehan and L. J. Whitman, "Detection limits for nanoscale biosensors," *Nano Lett.*, vol. 5, pp. 803–807, Apr. 2005.

Jae-Hyuk Ahn received the B.S. degree from the Department of Electrical Engineering, Korea Advanced Institute of Science and Technology, Daejeon, Korea, in 2007, where he is currently working toward the Ph.D. degree in electrical engineering.

His research interests include biosensors, nanofabrication technology, and characterization.

Sung-Jin Choi received the B.S. degree in electronics and electrical engineering from Chung-Ang University, Seoul, Korea, in 2007, and the M.S. degree from the Department of Electrical Engineering, Korea Advanced Institute of Science and Technology, Daejeon, Korea, in 2008, where he is currently working toward the Ph.D. degree in electrical engineering.

His current research interests include Schottky-barrier devices, capacitorless dynamic random-access memory, biosensors, and nanowire electronics.

Jin-Woo Han received the B.S. degree from the School of Information and Communication Engineering, Inha University, Incheon, Korea, in 2004, and the M.S. and Ph.D. degrees from the School of Electrical Engineering and Computer Science, Korea Advanced Institute of Science and Technology (KAIST), Daejeon, Korea, in 2006 and 2010, respectively.

He is currently a Postdoctoral Fellow at Center for Nanotechnology, NASA Ames Research Center, CA. His research interests include novel device, and nanofabrication technology, and his research covered a broad area in nanodevices ranging from device design to process development, simulation, characterization, and modeling.

Dr. Han led a research team responsible for developing the unified memory device "Unified-RAM (URAM)," in 2007, the nanoelectromechanical device "Fin Flip-flop Actuated Channel Transistor (FinFACT)," in 2009, and the gateless NPN nanowire device "Bistable Resistor (Biristor)," in 2010. He was the recipient of the best dissertation award from the KAIST in 2010.

Tae Jung Park received the B.S. and M.S. degrees from Chungnam National University, Daejeon, Korea, in 1998 and 2000, respectively, and the Ph.D. degree from the Department of Chemical and Biomolecular Engineering, Korea Advanced Institute of Science and Technology (KAIST), Daejeon, Korea, in 2008.

From December 1999 to May 2003, he was a Researcher with Daewoong Pharmaceutical Company and Bioventure Company in Korea, where he developed a protein engineering in microbes. He is currently an Adjunct Professor at the BioProcess Engineering Research Center , KAIST, and also the Vice Director of the Center for Nanobio Integration and Convergence Engineering, National Nanofab Center, Daejeon. He has authored or coauthored more than 70 papers, and holds 33 international patents as well as 30 Korean patents. His research interests include novel platform technologies for the nanobiofusion studies on the metal surface, biosensor chip and nanocomplex fabrication for electrochemical analysis as well as microfluidics, and an investigation of miniaturization and evaluation for the detection of optical and electrical signals.

Dr. Park received seven Best Research Awards from the Korean and international societies.

Sang Yup Lee received the B.S. degree from the Seoul National University, Seoul, Korea, in 1986, and the M.S. and Ph.D. degrees from the Department of Chemical Engineering, Northwestern University, Evanston, IL, in 1987 and 1991, respectively.

He is currently a Distinguished Professor and Dean of the College of Life Science and Bioengineering at Korea Advanced Institute of Science and Technology, Daejeon, Korea. He has authored or coauthored more than 370 papers, and holds 220 international patents as well as 230 Korean patents. He also has journal editorships from 19 international journals concerning applied biotechnology, systems biotechnology, and others. His research interests include metabolic engineering, biochemical engineering, and biosensor platform technologies.

Dr. Lee received 25 Research Awards from the Korean and international societies.

Yang-Kyu Choi received the B.S. and M.S. degrees from Seoul National University, Seoul, Korea, in 1989 and 1991, respectively, and the Ph.D. degree from the University of California, Berkeley, in 2001.

He is currently an Associate Professor with the Division of Electrical Engineering, Korea Advanced Institute of Science and Technology, Daejeon, Korea. From January 1991 to July 1997, he was a Process Integration Engineer with Hynix Semiconductor, Inc., Kyungki, Korea, where he developed 4M, 16M, 64M, and 256M DRAMs. He was involved in reliability physics and quantum phenomena for nanoscale CMOS. He has authored or coauthored more than 230 papers and is a holder of seven U.S. patents and 99 Korean patents. His research interests include multiple-gate MOSFETs, exploratory devices, novel and unified memory devices, nanofabrication technologies for bioelectronics, biosensors, and biomimesis.

Dr. Choi received the Sakrison Award for the best dissertation from the Department of Electrical Engineering and Computer Sciences, University of California, in 2002. He was also the recipient of "The Scientist of the Month for July 2006" from the Ministry of Science and Technology, Korea. His biographic profile was published in the 57th *Marquis Who's Who* in America.